IOSR Journal of Mechanical and Civil Engineering (IOSR-JMCE)
e-ISSN: 2278-1684, p-ISSN: 2320-334X, Volume 22, Issue 4 Ser. II (July - August 2025), PP 51-62
www.iosrjournals.org

Evaluating Soil Samples From The Vicinity Of The Great Benin Moat For Mud Brick Production And Pozzolanic Potential

John Audu, M.Eng., Sylvester Osuji, Phd
Department Of Civil Engineering, University Of Benin, Benin City, Edo State, Nigeria

Abstract
Traditional earthen materials and techniques offer a promising solution to the housing infrastructure crisis in Nigeria and sub-Saharan Africa. This exploratory study examines the chemical and physico-mechanical properties of soils used in mud buildings and the historic Benin moat in Benin City, Nigeria, with the aim of adapting them for modern, low-cost housing. Four soil samples were analyzed in raw form and with 5-10% cement and sodium hydroxide (NaOH) stabilization. At 14 days, cube strengths with 5% cement exceeded the 1.6 N/mm² requirement of the Nigerian Building Code (2006) for non-loadbearing sandcrete blocks by over 30%, while unconfined compressive strength (UCS) at 28 days was within 5-6% of the code. However, all samples failed the chloride ion penetration test. The samples met ASTM C618-22 oxide requirements ($SiO_2 + Al_2O_3 + Fe_2O_3 > 70\%$, $SO_3 < 4\%$, $K_2O < 1.5\%$) but showed high loss on ignition (LOI > 23%) and very low strength activity indices (<75%) at 28 days, limiting their pozzolanic performance. Despite this, the high kaolinite content (28–68%) suggests strong potential for producing metakaolin, a valuable supplementary cementitious material (SCM). While stabilized mud bricks - uncalcined - show promise at 5% cement, further chemical or mechanical treatment is needed to enhance durability and long-term performance.

Keywords: *Traditional earthen materials, mud buildings, Stabilized bricks, uncalcined, supplementary cementitious materials.*

Date of Submission: 14-08-2025 Date of Acceptance: 24-08-2025

I. Introduction

The Great Benin Kingdom, one of the most sophisticated precolonial civilizations in sub-Saharan Africa, left an enduring architectural legacy through its moats, walls, and traditional compounds. The monumental earthworks surrounding ancient Benin City collectively known as Iya were constructed using compacted clayey earth materials that were local sourced. These moats, which span thousands of kilometers, were originally meant to be military fortifications, but also symbolized their organizational and technological prowess (Idemudia, 2024). The samples analyzed in this study were collected from within the vicinity of these historic moats, providing us with an opportunity to explore the engineering embedded in traditional African soil construction. Much of the moat's original grandeur has been lost over time due to centuries of erosion and recent encroachment by urban development. Fig. 1 shows a picture of a small portion of what presently remains of the Benin Moat.

Fig. 1. Part of The Remains of The Benin Moat (Source: The Centenary Project / Google Arts & Culture).

In addition to the moats, Benin's indigenous architecture was dominated by earthen buildings - structures made with mud bricks, clay plasters, and thatched roofing systems. These buildings adapted quite well to the tropical climate, they were easy to repair, and environmentally friendly.

This exploratory study aims to characterize and assess the engineering properties of traditional mud samples collected from Benin City, Nigeria, specifically evaluating their potential for uncalcined, minimally processed bricks and supplementary cementitious materials (SCMs). These materials, if properly understood, can replace or reduce the use of Ordinary Portland Cement (OPC) in non-loadbearing construction, resulting in lower emissions, lower costs, and more regionally adapted infrastructure framework. Despite being exploratory, the research employs standard evaluation techniques to examine their pozzolanic characteristics and determine suitability for sustainable building applications as discussed by Scrivener et al. (2018). As Pachta et al. (2014) explain, the use of mud mortars and sun-dried bricks goes back as far as 8000 BC. The sheer scale and durability of constructs like the Benin moats are a glowing testament to the engineering proficiency of African builders of old without the benefit of the OPC of today.

Artioli and Secco (2016) describe the composition of ancient earthen walls, which were created by stacking mud bricks and sealing them with a moist layer of clay that dried into a hardened mass. Such a system leveraged natural cohesion, required no high-temperature processing, and, most importantly, could be easily repaired and/or reused. Unfortunately, with the emergence of Portland cement in the 19th century, these methods lost prominence due to the shorter setting time and early strength offered by cement (Shi, 2001). Nonetheless, this modern alternative comes at significant environmental cost, as cement manufacturing is responsible for 5-8% of global CO_2 emissions (Azad et al., 2013; Andrew, 2018). This is in addition to the emvironmentl degradation from overly scarifying borrow pits for materials deemed more suitable for modern use, and hauling them through long distances.

Fig. 2 is a picture of a typical traditional hut and an adaptation of traditional materials/methods for constructing a colonial-style building more than 50 years ago. With a pressing housing deficit of over 20 million homes by some accounts, Nigeria needs to re-evaluate traditional building materials and techniques for their inherent potential. This offers a compelling path toward affordable and culturally rooted housing solutions that are scalable (Adedeji et al., 2023). Moreover, the use of these materials supports environmental goals by reducing reliance on Ordinary Portland Cement (OPC), which is said to be responsible for approximately 8% of global CO_2 emissions (Andrew, 2018).

Fig. 2. Traditional Hut and Colonially Influenced Adaptation (Sources: iStock, 2025, File ID: 1290323614).com; Storey building – Courtesy, Wole Abu, 2024)

A recent study explores the physical and mechanical properties of soils in Benin, particularly in relation to their geotechnical and agricultural potential. Dayou et al. (2017) assessed soil resistance across Benin's agroecological zones, revealing that many soils, specially in the southern regions, are sandy loams with moderate compaction and good drainage. These characteristics are favorable for construction when stabilized. A simlar study by Kpade et al. (2022) developed a digital soil fertility index map for Benin using available data and machine learning, and identified key soil properties . While these studies were not construction-focused, they provide valuable baseline data on the chemical and mineralogical variability of Benin soils. This study builds on this foundation by focusing specifically on the pozzolanic potential and the suitability for contemporary mud brick production of traditional building muds from Benin.

In terms of practical applications, the use of uncalcined, minimally processed (UMP) traditional muds as partial cement replacements or stabilizers represents a tangible solution to both the climate and housing crises. Cardoso et al. (2022) point to the need for new sources of aluminosilicates to supplement SCM stocks, emphasizing that materials should be abundant and sourced locally to ensure ecological and economic sustainability. The samples analyzed in this work from Benin match these criteria. However, further studies are required to standardize processing techniques, improve consistency in performance metrics, and promote wider adoption of these age-old, yet now crucially modern, building solutions.

Importantly, this study proposes a cheaper and safer low-carbon alternative to conventional bricks/blocks: uncalcined, air-dried mud bricks, made from the abundant clay-rich soils that dominate the landscape. Stabilizing these bricks with 5-10% cement or NaOH could potentially result in fit-for-purpose bricks while reducing the use of cement. Note that in Nigeria, sandcrete blocks are typically produced at a 1:6 to 1:8 cement-to-sand mix ratio by volume, which corresponds to cement content of about 10 wt.% (or higher) and strengths between 1.73 N/mm² at 7 days and 2.39 N/mm² at 28 days (Oyelade et al., 2025; Wenapere & Ephraim, 2009). This informed the mix ratios selected for this study with the prize being to succeed with the lower cement content. It is noteworthy that Nigeria National Building Code stipulates a minimum 14-day compressive strength of 1.6 N/mm² for sandcrete blocks intended for use in non-load-bearing walls of single-storey buildings, in line with NIS 87:2004.

Some cement chemistry nomenclature are adopted for this study: calcium oxide (CaO) is abbreviated to C, silicon dioxide (SiO_2) to S, aluminium oxide (Al_2O_3) to A, and iron(III) oxide (Fe_2O_3) to F (Dodson, 1990); while water (H_2O) is denoted H, magnesium oxide (MgO) as M, potassium oxide (K_2O) as K, and sodium oxide (Na_2O) as N (Elsen et al., 2011). The reactivity of supplementary cementitious materials (SCMs) is governed by several interrelated factors, including their chemical composition, particle fineness, presence of glassy or amorphous phases, as well as the pH and temperature conditions during hydration (Geiker and Gallucci, 2019). For example, silica-rich SCMs tend to modify the calcium-to-silicon (Ca/Si) ratio in calcium silicate hydrate ($CaO\text{-}SiO_2\text{-}H_2O$, commonly denoted C–S–H) gels, while those with higher alumina content promote the formation of calcium aluminate hydrates ($CaO\text{-}Al_2O_3\text{-}H_2O$, or C-A-H), contributing to altered mechanical and durability characteristics in cementitious systems. Furthermore, the incorporation of micro- and nano-sized particles can lead to more homogeneous and finer pore structures in cement paste, possibly due to the nucleation and growth of C-S-H phases on these particles (Geiker and Gallucci, 2019). In stabilized soils, strength is gained via the hydration of cement compounds in the presence of water, specifically dicalcium silicate ($2CaO\cdot SiO_2$, or C_2S) and tricalcium silicate ($3CaO\cdot SiO_2$, or C_3S), alongside the pozzolanic reaction involving calcium hydroxide [$Ca(OH)_2$] and the active minerals in the soil (Sherwood, 1993; Makusa, 2012).

Judging good pozzolan according to ASTM C618 - Standard Specification for Coal Fly Ash and Raw or Calcined Natural Pozzolan for Use in Concrete - dictates the key requirement for Class N (Natural Pozzolan as shown in Table 1. The Turkish standard also adopts the same criterion for evaluating good pozzolanic materials. This assessment to ascertain the pozzolanicity of a natural pozzolan is a requirement in the cement industry, and it is generally accepted that natural pozzolans containing lower quantities of clay minerals and abundant zeolitic phases demonstrate enhanced pozzolanic activity, particularly those with $SiO_2 + Al_2O_3 \geq 80\%$ and subdued levels of MgO and SO_3 (Alp et al., 2009). So, while this statement applies to some natural pozzolans, materials rich in kaolinite – a type of clay - are also highly reactive when thermally activated.

Table 1. ASTM C618-12 requirements for class N Pozzolans.

SN	Constituents	Requirements
1	$SiO_2 + Al_2O_3 + Fe_2O_3$	Minimum of 70%
2	SO_3	Maximum of 4%
3	Moisture content	Maximum of 3%
4	Available Alkalis (Na_2O, K_2O)	Maximum of 1.5%
5	Loss on ignition (LOI)	Maximum of 10%
6	Residue (percentage retained on 45µm sieve); measure of fineness	Maximum of 34%
7	Strength activity of cement (SAI)	Minimum of 75%

(adapted from (Ayininuola and Adekitan 2016))

ASTM C618 has long been regarded as the benchmark for evaluating the suitability of natural pozzolans in concrete applications. However, comparative studies reveal that its performance metrics, particularly the Strength Activity Index (SAI), do not always align when tested against standards from the European Union, Canada, China, and India (Rios et al., 2021). Rios et al. (2021) highlight that some ASTM C618 SAI requirements can also be met by non-pozzolanic materials, raising concerns about the validity of compressive strength as a sole indicator of pozzolanic reactivity. In addition, ASTM C618 has been critiqued for its rigidity in accommodating emerging/ alternative sources of pozzolanic materials, possibly limiting innovation in SCM development (Rios et al., 2021).

Researchers have been exploring innovative alternatives to Ordinary Portland Cement (OPC), with a growing interest in alkali-activated concrete (AAC) using natural pozzolans. A study by Ibrahim et al. (2018) investigated the use of natural pozzolans as precursors for AAC, finding that a sodium silicate to sodium hydroxide (SS/SH) ratio of 2.5 and a 14 moles/liter NaOH solution yielded optimal strength and microstructural properties. The study examined various SS/SH ratios and NaOH molarities, conducting compressive strength tests over 0.5 to 28 days at 60 °C. Microstructural analysis via SEM, Energy Dispersive Spectroscopy (EDS), and XRD revealed the formation of dense, well-bonded matrices under optimal conditions. In a related study, Mota et al. (2018) investigated the impact of NaOH and Na_2SO_4 on white cement hydration kinetics. Their findings revealed that NaOH accelerates early hydration but negatively affects long-term strength development. In contrast, Na_2SO_4 enhances sustained strength gain by promoting ettringite formation and reducing porosity. However, the widespread adoption of alkali-activated concrete (AAC) using sodium-based activators, such as NaOH, is hindered by concerns over their high cost, corrosiveness, and environmental implications (Guo et al., 2023).

II. Materials And Methods

To adequately characterize soil samples, a suite of tests is required.All laboratory tests were conducted in accordance with relevant ASTM standards for soil and concrete materials (ASTM International, 2021–2025). The tests for measuring pozzolanicity index include, but not limited to the following: X-ray diffractometry (XRD) and thermogravimetric analysis (TGA), X-ray fluorescence spectrometry (XRF), Frattini test, FAST, modified Chapelle, determination ozzolanic activity through electrical conductivity, R3 (Rapid, Relevant, Reliable), colorimetry (Alujas et al. 2015; Pinheiro et al. 2023). Broadly, tests for pozzolanic reactivity may be grouped into mechanical, thermal and chemical tests, and multiple tests are usually deployed to achieve reliable results (Pinheiro et al. 2023).

Chemical analyses such as XRF and XRD are essential for determining elemental composition and mineral phases (Ayininuola & Adekitan, 2016). Scanning Electron Microscopy (SEM) offers critical insights into particle morphology and microstructural features, while TGA is used to assess thermal stability and loss on ignition - both key indicators of pozzolanic activity. These complementary tests help determine whether materials satisfy the criteria for pozzolans used in SCMs as outlined in ASTM C618-22 - and predict how they might perform under thermal or mechanical stress conditions.

In addition to chemical and thermal tests, physical and mechanical evaluations are critical. These include particle size distribution (sieve analysis), Atterberg limits (to determine plasticity), moisture content, and compaction characteristics such as maximum dry density (MDD) and optimum moisture content (OMC). The unconfined compressive strength (UCS) test, as outlined in ASTM D2166, is particularly important for assessing the load-bearing capacity of stabilized samples. When used in combination, these tests provide a holistic understanding of the material's behavior and suitability for construction applications.

Sample Collection

Four representative samples labelled BEN1a, BEN1b, BEN2a, and BEN2b were collected from two traditional locations in Benin City – Uselu and Ikpoba Hill areas– at coordinates 6.311421°N, 5.500540°E (BEN1a/b) and 6.431547°N, 5.603254°E (BEN2a/b) respectively. The samples were collected at depths of about 2 ft below the ground to avoid the horizon with organic matter (Minke 2005). For the cement stabilization experiments, Portland Limestone Cement was employed, specifically SOKCEM II-42.5N, manufactured by BUA Cement at their plant in Sokoto State, Nigeria in accordance with NIS 444-1: Composition, specifications and conformity criteria for common cements.

Experiments and Sample Preparation

The soil samples were initially air-dried, pulverized, and sieved to ensure consistency and uniformity. Chemical and microstructural analyses were performed using XRD, XRF, and SEM (Iorfa et al. 2020; Moussa et al. 2022). XRD analysis was conducted using a Rigaku MiniFlex benchtop diffractometer to investigate the microstructure and identify mineral phases within the samples. This technique relies on the diffraction of X-rays off crystal planes, producing unique patterns that correspond to specific minerals based on their atomic structure. Such identification is critical in soil mineralogy, particularly for detecting clay minerals that influence soil plasticity and stability. Sample preparation for XRD followed ASTM guidelines, including ASTM E691, and involved grinding to reduce particle size, sieving for uniformity, oven-drying at 100 °C for 2 hours to remove moisture, centrifugation to isolate the clay fraction, and preparing oriented mounts for clay-specific analysis. Approximately 1.5 grams of material were used per sample. The analysis employed Cu-Kα radiation ($\lambda = 1.54056$ Å), with scans performed over a 2θ range of 3.00° to 70.00° at 0.02° intervals, allowing for high-resolution peak detection (Moussa et al., 2022). Resulting diffraction patterns were matched against entries from the International Centre for Diffraction Data (ICDD) to aid in mineral phase identification. Fig. 3 depicts the sample collection, air-drying on tarps, labelling and preparation for chemical tests.

Fig. 3. Sample Collection and Preparation for Chemical Tests

The chemical composition of the untreated soil samples was determined using Xenemetrix's Genius IF (Secondary Targets) Energy-Dispersive X-Ray Fluorescence (EDXRF) spectrometer. SEM analyses were carried out using the Oxford PhenomProx. Scanning Electron Microscopy (SEM) offers high-resolution imaging to study soil microstructure, particle morphology and bonding in soils, particularly those with unique mineralogical characteristics. TGA were performed using PerkinElmer MES-TGA TGA4000 brand, manufactured in the Netherlands. TGA measures soil weight loss or thermal decomposition under controlled heating, identifying moisture, organic content, and mineral stability. Different materials lose weight at specific temperatures, revealing compositional changes.

For the particle size distribution, both dry and sedimentation analysis were done to adequately capture the full range of particle sizes per the requirements of ASTM D 6913. For the Atterberg limits and related tests, ASTM D 4318 was used in conjunction with ASTM D 698. BS 1377 (British Standards Institution, 1990) and ASTM D2166 (2010), which specify methods for evaluating soil properties and determining the unconfined compressive strength of cohesive soils, respectively. The Manual of Soil Laboratory Testing Vol. 1 (Head, 2006) was also consulted. Fig. 4 shows some pictures of the actual UCS tests in progress. The equipment used for conducting the UCS tests includes: an automatic loading machine with a maximum capacity of 50 kN. UCS and required compaction were carried out in accordance with the requirements of BS 1377. UCS is a widely used test for evaluating the strength of stabilized soils, particularly when assessing improvements from additives like cement. It provides a direct measure of how well the soil resists axial compression without lateral support, making it ideal for geotechnical applications. This method is especially valuable for calculating the Strength Activity Index (SAI), which compares treated and untreated samples to quantify stabilization effectiveness, as demonstrated by Wang et al. (2024).

Fig. 4. UCS Tests in Progress

Cube tests were also conducted on the samples: Concrete cubes of size **150×150×150 mm** were tested for compressive strength in accordance with **BS EN 12390-3** (British Standards Institution, 2019). These cubes were cured under standard conditions and tested at **7 and 14 days** to monitor strength development. Typically, concrete achieves about 65–70% of its 28-day strength at 7 days, and around 85–90% by 14 days (HowToConcrete.com, 2025).

Chloride-ion penetration test was carried out in line with the requirements of ASTM C1202 using the Norton Clipper CFW 0251 manufactured by Norton Construction. It has a spindle speed of 3250 RPM. The air-dried cubes (samples) were immersed in a prepared Sodium chloride solution (35%) for Twenty-eight (28) days to allow chloride ions to penetrate therefore simulating a marine-like chloride concentration.

III. Results

Chemical & Thermal Tests

Running the XRD based on the base data previously provided, Table 1 provides details of the key parameters derived from the XRD. BEN1a shows 4 peaks while all other samples displayed 5 main peaks. The table presents key parameters used in XRD analysis to characterize soil mineralogy. The 2θ (°) column indicates the diffraction angle where peaks occur, while d (Å) represents the interplanar spacing calculated via Bragg's Law. Height (cps) refers to the peak intensity in counts per second, which reflects the relative abundance of the corresponding phase. FWHM (°2θ), or Full Width at Half Maximum, measures peak broadening and is used to assess crystallinity and estimate particle size. Int. I. (cps·°) denotes the integrated intensity of a diffraction peak and represents the total area under the peak by combining its height and width. This provides a more comprehensive measure of phase concentration than peak height alone. Size (Å) provides an estimate of crystallite dimensions derived from peak broadening using the Scherrer equation. Phase(s) identifies the mineral or crystalline phase associated with each peak, and ICDD PDF lists the reference code from the International Centre for Diffraction Data used for phase identification.

Table 1. Key Peak Parameters

2θ (°)	d-spacing (Å)	Height (cps)	FWHM (°)	Int. I. (cps·°)	Size (Å)	Mineral Phase	ICDD Card No.
BEN1a							
12.5	7.07	320 ± 25	0.42 ± 0.07	175 ± 26	197 ± 34	Kaolinite-1A	01-080-0886
20.2	4.385	285 ± 28	1.25 ± 0.12	380 ± 64	67 ± 7	Kaolinite-1A + Orthoclase	01-080-0886, 00-002-0475
24.9	3.567	356 ± 24	0.28 ± 0.07	136 ± 26	302 ± 75	Kaolinite-1A	01-080-0886
26.7	3.333	4186 ± 594	0.13 ± 0.02	610 ± 62	682 ± 133	Quartz + Kaolinite-1A	01-086-2237, 01-080-0886
BEN1b							
12.8	6.93	235 ± 36	0.44 ± 0.08	127 ± 24	192 ± 35	Kaolinite	00-001-0527
21.2	4.19	352 ± 36	2.8 ± 0.3	1892 ± 224	30 ± 3	Quartz + Orthoclase	01-073-6618, 00-002-0475
25.4	3.51	210 ± 25	1.3 ± 0.2	305 ± 138	67 ± 12	Kaolinite + Orthoclase	00-001-0527, 00-002-0475
27.1	3.286	3975 ± 199	0.11 ± 0.01	600 ± 24	749 ± 59	Quartz + Albite	01-073-6618, 00-003-0451
37.1	2.42	155 ± 16	1.11 ± 0.19	202 ± 32	79 ± 14	Quartz + Orthoclase	01-073-6618, 00-002-0475
BEN2a							
12.8	6.93	235 ± 36	0.44 ± 0.08	127 ± 24	192 ± 35	Kaolinite	00-001-0527
21.2	4.19	352 ± 36	2.8 ± 0.3	1892 ± 224	30 ± 3	Muscovite	00-001-1098
25.4	3.51	210 ± 25	1.3 ± 0.2	305 ± 138	67 ± 12	Orthoclase	00-019-0931
27.1	3.29	3975 ± 199	0.11 ± 0.01	600 ± 24	749 ± 59	Quartz	01-073-6618
37.1	2.42	155 ± 16	1.11 ± 0.19	202 ± 32	79 ± 14	Albite	00-003-0451
BEN2b							
12.4	7.12	606 ± 59	0.29 ± 0.06	324 ± 24	284 ± 55	Kaolinite	00-001-0527
20.8	4.26	425 ± 45	2.4 ± 0.2	1853 ± 125	35 ± 3	Muscovite	00-001-1098
24.1	3.7	513 ± 51	0.12 ± 0.05	80 ± 18	713 ± 287	Goethite	00-001-0401
24.9	3.57	423 ± 39	0.78 ± 0.11	435 ± 76	108 ± 15	Orthoclase	00-019-0931
26.7	3.34	4136 ± 208	0.13 ± 0.01	677 ± 27	684 ± 50	Quartz	01-073-6618

Table 2 shows the results of the XRD trace for BEN1a, BEN1b and BEN2a, BEN2b respectively obtained from the peaks points shown on Table 1. It represents the results of the XRD analysis showing the minerology and the content (wt. %) of the various phases. Quartz is present in all the samples from quantities

ranging from relatively low (BEN1a - 11.46%) to relatively high (BEN2b - 46%). Kaolinite is present in all the samples with BEN2a being the lowest at 19% and BEN1a, the highest at 66.4%.

Table 2. Mineral Composition Results for BEN1a, BEN1b, BEN2a, and BEN2b

Sample	Kaolinite (%)	Quartz (%)	Orthoclase (%)	Albite (%)	Muscovite (%)	Goethite (%)
BEN1a	66.40 ± 3	11.46 ± 11	9.22 ± 9	6.17 ± 6	6.75 ± 7	–
BEN1b	42.00 ± 8	33.00 ± 13	5.00 ± 10	16.00 ± 3	4.20 ± 8	–
BEN2a	19.00 ± 7	37.00 ± 5	13.10 ± 14	21.00 ± 2	4.60 ± 5	4.80 ± 5
BEN2b	39.00 ± 2	46.00 ± 2	9.60 ± 5	2.80 ± 5	0.70 ± 4	0.90 ± 6
Formula	$Al_2Si_2O_5(OH)_4$	SiO_2	$KAlSi_3O_8$	$NaAlSi_3O_8$	$H_2KAl_3(SiO_4)_3$	$Fe_2O_3 \cdot H_2O$

Fig. 5 shows the **s**uperimposed XRD patterns of **BEN1a, BEN1b, BEN2a, and BEN2b** with intensities **normalized within 0–100**, representing the full XRD trace for the samples over the 2θ range. Vertical markers label diagnostic reflections as shown on Table 1.

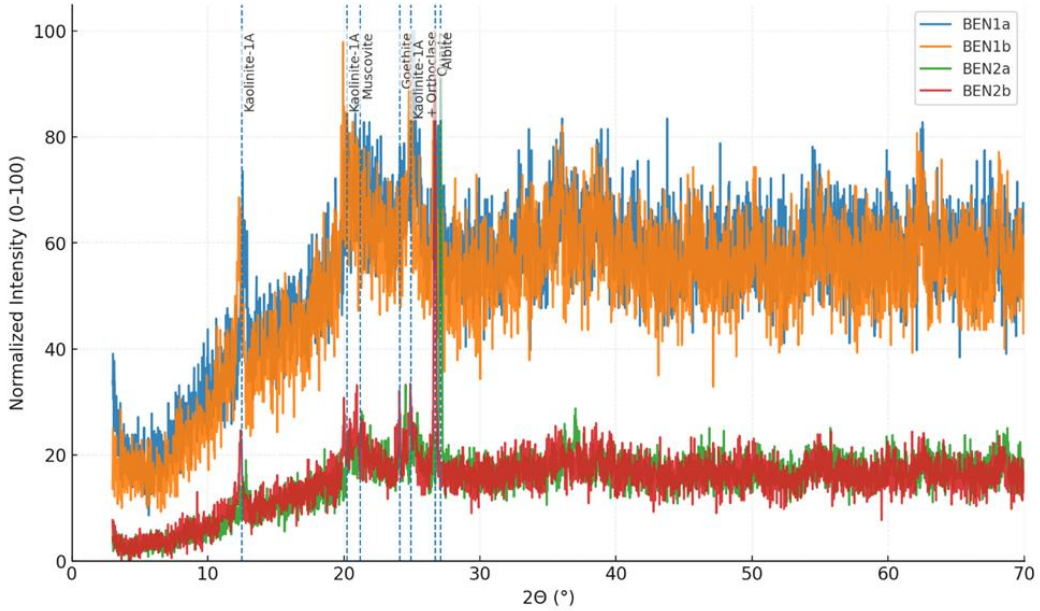

Fig. 5. Mineralogical Phases from XRD Results for BEN1a, BEN1b, BEN2a, BEN2b

Further deductions may be made from the results of the XRF shown in Table 3 which contain the elemental and chemical compositions side by side. The oxide composition table quantifies key chemical constituents in SCMs - primarily silicon dioxide (SiO_2), aluminium oxide (Al_2O_3), and iron(III) oxide (Fe_2O_3) - which are critical for pozzolanic activity and material classification. Calcium oxide (CaO) and sulphur trioxide (SO_3) influence hydration and setting, while minor components like magnesium oxide (MgO), potassium oxide (K_2O), and chlorine (Cl) affect durability. However, this table does not reveal how these oxides are structurally arranged, which is what the XRD results of Table 1, Fig. 5, and Table 2 displayed. Together, they provide a complete picture of SCM performance. There is a relationship between the XRD results and the chemical constituents is evident from the data presented.

Table 3. Elemental and Chemical Compositions of BEN1a and BEN1b from XRF

Element (E)	Oxide (O)	BEN1a (E/O)	BEN1b (E/O)
Si	SiO_2	16.090 / 34.421	22.805 / 48.787
Al	Al_2O_3	11.815 / 22.323	15.535 / 29.353
Fe	Fe_2O_3	16.983 / 24.281	10.270 / 14.683
Ca	CaO	2.235 / 3.127	0.491 / 0.687
S	SO_3	0.080 / 0.200	0.084 / 0.209
Mg	MgO	0 / 0	0 / 0
K	K_2O	0.550 / 0.663	0.437 / 0.527
Cl	Cl	9.501 / 9.501	1.904 / 1.904
-	**S+A+F**	**- / 81.025**	**- / 92.823**

While the XRD tells how the samples are structured mineralogically and the XRF shows what chemicals are in it, Fig. 6 depicts the SEM, which displays what the samples look like magnified to x500 and x2000. The samples are irregularly shaped with variable sizes. The SEM images of BEN1a revealed irregular, angular particles with a combination of plate-like and blocky morphologies (Mitchell and Soga, 2005). In contrast, the SEM image of BEN2 also displayed irregular shapes with similar features, but with a greater presence of dispersed fine particles. Morphology and particle packing revealed by SEM are indicative of surface area availability and microstructural accessibility, both of which influence reactivity and hydration kinetics.

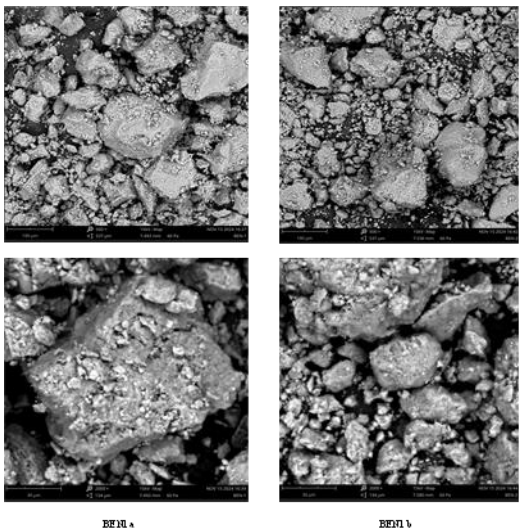

Fig. 6. SEM Surface Morphology and Microstructure for BEN1a and BEN1b

The thermogravimetric analysis (TGA) revealed that all the samples had Loss on Ignition (LOI) of > 10%. There were distinct thermal behaviors linked to their mineralogy: For BEN1a, minimal mass loss was observed up to 600°C, which was mainly attributed to the evaporation of physically bound water. However, between 600°C and 850°C, a significant 55% weight loss occurred. In contrast, BEN1b displayed an earlier onset of decomposition: substantial weight loss began from 250°C to 500°C (about 90%), followed by a gradual reduction up to 700°C.

Chloride-ion Penetration Test

The chloride penetration test was performed on the samples to evaluate their resistance to chloride ingress after exposure to concentrated saline conditions. Only the 10% cement-stabilized samples remained intact for testing, as all other cubes crumbled, signifying their vulnerability to chloride-induced degradation. **BEN1a** showed *light chloride penetration*, with minimal silver chloride precipitate formation, indicating strong resistance and better durability for reinforced applications. In contrast, **BEN1b** exhibited *deep chloride penetration*, with visible white precipitate extending beyond **25 mm**, suggesting high porosity and a significant risk of steel corrosion without further stabilization. These results underscore the variability in performance even within samples from the same region.

Physio-mechanical Tests

Soil Classification Tests and Moisture Content

Sieve analyses and Atterberg limits tests were carried out for all the samples to aid in their classification, and to examine their gradation. Optimum moisture content was also determined. These laboratory analyses revealed a range of properties. Fig. 7 shows the PSD curves for BEN1a, BEN1b, BEN2a, and BEN2b, and the associated table.

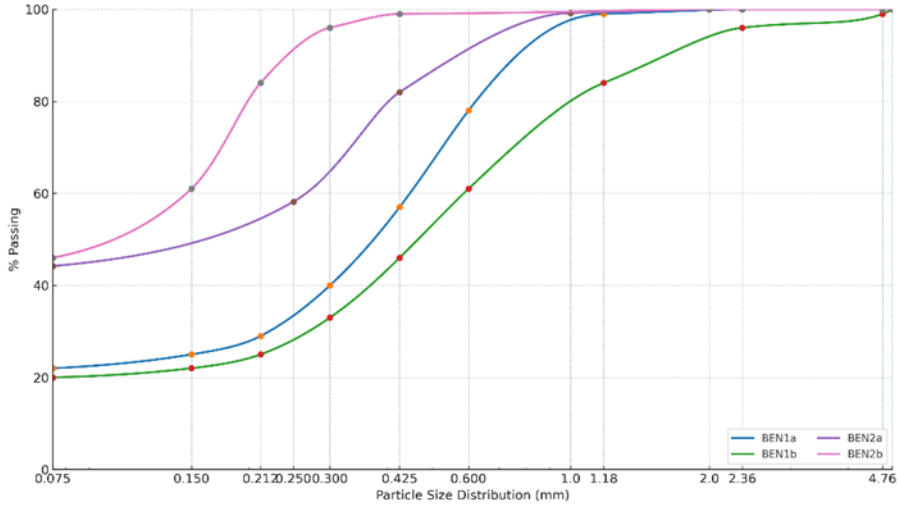

	0.075	0.150	0.212	0.250	0.300	0.425	0.600	1.0	1.18	2.0	2.36	4.76	5.0
BEN1a	22.0	25	29	-	40	57	78	-	99	-	100	100	100
BEN1b	20.0	22	25	-	33	46	61	-	84	-	96	99	100
BEN2a	44.2	-	-	58.2	-	82	-	99.2	-	100	100	100	100
BEN2b	46.0	61	84	-	96	99	-	-	-	100	100	100	100

Fig. 7. Particle Size Distribution Curves

Table 4 presents the outcomes of the Atterberg Limit and compaction tests, which serve as key indicators for soil classification and contribute to the selection of appropriate trial mixes, among other engineering considerations.

Table 4. Physical Properties and Soil Classification of BEN1a and BEN1b

Sample	LL (%)	PL (%)	PI (%)	LS (%)	MDD (g/cm^3)	OMC (%)	USCS Classification
BEN1a	33	17	16	3	1.93	11	Clayey sand (SC)
BEN1b	39	16	23	5	1.95	11	Clayey sand (SC)

Abbreviations: LL: Liquid Limit. PL: Plastic Limit. PI: Plasticity Index. LS: Shrinkage Limit.

Unconfined Compressive Test (UCS)

UCS results for 7, 14, and 28-day results are shown in Table 5 for the various stabilization methods.

Table 5. 7, 14, 28-Day UCS Results in kPa

Stabilization	7-Day		14-Day		28-Day	
	BEN1a	**BEN1b**	**BEN1a**	**BEN1b**	**BEN1a**	**BEN1b**
0%	69	61	100	109	134	136
5% NaOH	74	67	113	141	158	164
10% NaOH	144	144	157	158	207	158
5% Cement	405	388	570	478	1514	1521
10% Cement	267	256	778	603	2120	1952

To compare the results of the UCS, some Cube Strength tests were carried out, which are shown in Table 6 for the BEN2 samples.

Table 6. 7 & 14-day cube strength results for BEN2a and BEN2b in KPa

Stabilization	Sample	7-Day Strength	14-Day Strength
0% Additive	BEN2a	200	200
	BEN2b	200	200
5% Cement	BEN2a	1700	2100
	BEN2b	1900	2500
10% Cement	BEN2a	2400	3100
	BEN2b	2500	3300
5% NaOH	BEN2a	500	1100

	BEN2b	600	1400
10% NaOH	BEN2a	1700	2100
	BEN2b	1800	2100

IV. Discussion

BEN1a (66.4%) and BEN1b (42%) are characterized by high kaolinite content, which is a key indicator of potential pozzolanic reactivity when thermally activated (Ayininuola and Adekitan, 2016). In contrast, BEN2a (19%) exhibits significantly lower kaolinite and higher quartz content of 37%, suggesting a more inert nature. BEN2b, with 39% kaolinite and 46% quartz, lies between BEN1a/b and BEN2a in terms of reactivity and structural contribution. See Table 2. The high quartz content in BEN2 samples can serve as mechanical fillers, enhancing particle packing and stability, though it contributes little to chemical reactivity. All samples contain combined $SiO_2 + Al_2O_3 + Fe_2O_3$ (S+A+F) values exceeding 70%, satisfying the oxide composition criterion of ASTM C618-22 for Class N pozzolans, as shown in Table 3. Although other samples exhibit low CaO levels (<3%), BEN1a shows a slightly higher content (3.127%), suggesting that while external activation may be necessary for the others, BEN1a could possess marginal self-cementing potential. This interpretation aligns with findings by Rashad (2023), who noted that CaO levels around 3% *may* contribute to early strength development in alkali-activated materials, even if not sufficient for full activation, depending on curing method and activator type.

Thermal analysis via TGA supports this interpretation. BEN1a shows a distinct dehydroxylation event between 600°C and 850°C, consistent with the transformation of kaolinite into metakaolin, which is a highly reactive pozzolanic phase. BEN1b, on the other hand, exhibits substantial weight loss between 250°C and 500°C, followed by gradual decomposition up to 700°C. This might point to a wider, but potentially less efficient transformation, possibly involving other phases with volatile materials. These thermal behaviors align with the mineralogical data from XRD, which confirms the dominance of kaolinite and quartz, and with SEM observations that reveal irregular, angular morphologies in BEN1a and finer, more dispersed grains in BEN1b. Such microstructural features influence both reactivity and mechanical interlock (Mitchell and Soga, 2005).

The relationship between crystallite size from XRD and particle size distribution (PSD) is also evident. Larger crystallite sizes (e.g. 682 Å for quartz in BEN1a) correspond to coarser fractions retained on sieves above 425 µm, while finer kaolinite phases (67–197 Å) align with the clay-sized fractions passing the 75 µm sieve. This correlation reinforces the structural interpretation of the soil matrix and supports the classification outcomes. Similar relationships have been documented in soil mineralogy studies (Zhang et al., 2022; Pan et al., 2025), where XRD peak widening and the dimensions of PSD fractions jointly inform soil texture and reactivity.

From the PSD results, all four samples exhibit a wide range of particle sizes but retain a considerable proportion above the 75 µm sieve. According to the Unified Soil Classification System (USCS), a soil is classified as SC (Clayey Sand) when over 50% passes through the No. 4 sieve (4.75 mm), more than 12% passes the No. 200 sieve (75 µm), and the material exhibits plasticity. Kaolinite contributes to the clay fraction, while quartz and feldspars like orthoclase and albite remain in coarser size ranges. BEN2a and BEN2b, with increased quartz content and higher sand fractions, show granular textures and larger voids in SEM imagery. Despite this, they still meet the fines and plasticity criteria for SC classification.

Mechanical performance was assessed through UCS and cube strength tests. Using the Nigerian Industrial Standard (NIS 87:2007) and Ontario's Building Code (2012), which stipulate minimum compressive strengths of 2500 kPa for non-load bearing sandcrete blocks, we find that none of the samples meets this threshold in their raw state stabilization. And, even with stabilization, the UCS at 5% cement content still does not pass. However, at 10% cement, BEN1a reaches 2120 kPa and BEN1b 1952 kPa, yielding Strength Activity Index (SAI) values of 84.8% and 78.1% respectively, which comfortably surpasses the ASTM C618-22 benchmark of 75%. More importantly, this study emphasizes the viability of 5% cement stabilization as a more environmentally sustainable alternative. At 5% cement, BEN1a and BEN1b achieve UCS values of 1514 kPa and 1521 kPa, respectively. While these fall short of the 2500 kPa requirement, they are reasonably close to the more lenient 1600 kPa benchmark from the Nigeria National Building Code (NBC, 2006) - both 5% and 10% cement-stabilized samples pass comfortably. It is important to note that 10% cement stabilization is closer to customary practice in subgrade improvement and block production (Gross and Adaska, 2020), but 5% offers a more environmentally friendly alternative with acceptable performance.

Cube strength tests for BEN2a and BEN2b further support this conclusion. At 14 days and 10% cement, both samples exceed 3000 Kpa, which surpasses the Ontario Building Code's requirement of 2.5 MPa for non-load bearing blocks and aligns with NIS 87:2007. These findings suggest that even less reactive samples, when properly stabilized, can meet performance benchmarks for low-load applications.

Durability assessments via chloride-ion penetration tests show that only the 10% cement-stabilized samples remained intact after 28 days in saline solution. BEN1a demonstrated minimal ingress, while BEN1b

showed deeper penetration, consistent with its finer morphology and higher porosity. These results align with SEM observations and further validate the need for adequate stabilization in aggressive environments.

Lastly, NaOH showed no appreciable gain in UCS tests even at 10%, but the cube strength results were quite promising across the range of 5-10 wt.%, with 10% being above NBC's 1600 Kpa and within 20% of 2500 KPa stipulated by NIS 87:2007. This is consistent with Iravanian (2022) who mentioned an optimal mix ration of 15% as opposed to the 5-10% used here. Besides, NaOH is not cost-effective in Nigeria currently.

V. Conclusion

This exploratory study has demonstrated the promising potential of locally sourced clays from Benin City for both earthen stabilized block production and supplementary cementitious material (SCM) development. BEN2a and BEN2b exhibited strong mechanical performance in mud brick applications, particularly when stabilized with the more environmentally friendly 5% cement, while BEN1a and BEN1b showed significant pozzolanic activity post-calcination, indicating their viability as SCMs.

Importantly, this research not only advances sustainable construction practices but also reinforces the historical significance of these materials in indigenous engineering. The Great Benin Moat - one of the largest man-made earthworks in history - was constructed using similar clay-rich soils without the aid of modern binders. Its enduring structure likely benefited from the high plasticity and cohesive strength of the native clays, prolonged curing times, and consistent maintenance practices that have been lost with time and urbanization. These findings validate the material choices of ancient builders and highlight the relevance of traditional knowledge in contemporary low-carbon construction.

Future studies could enhance the durability and strength of mud bricks. These studies may include fibre reinforcement, surface treatments, impact of nanomaterials, AAC optimization, the impact of additional mechanical/chemical enhancements, and accelerated aging tests. Likewise, optimizing SCM activation via alternative thermal profiles or alkali activation could reduce energy demands and broaden the applicability of BEN1 clays. Field trials, microstructural analysis, and life-cycle assessments will be essential to validate these materials under real-world conditions and scale their use effectively.

Overall, the findings lay a solid foundation for advancing low-carbon, locally sourced building materials that align with both environmental and cultural heritage goals.

References

[1] Adedeji I, Deveci G, Salman H (2023) The Challenges In Providing Affordable Housing In Nigeria And The Adequate Sustainable Approaches For Addressing Them. Open Journal Of Applied Sciences 13:431–448. Https://Doi.Org/10.4236/Ojapps.2023.133035

[2] Alp I, Deveci H, Süngün Y, Yılmaz A, Kesimal A, Yilmaz A (2013) Pozzolanic Characteristics Of A Natural Raw Material For Use In Blended Cements. Iranian Journal Of Science And Technology, Transaction B: Science 33:291–300

[3] Alujas A, Fernández R, Quintana R, Scrivener KL, Martirena F (2015) Pozzolanic Reactivity Of Low Grade Kaolinitic Clays: Influence Of Calcination Temperature And Impact Of Calcination Products On OPC Hydration. Applied Clay Science 108:94–101. Https://Doi.Org/10.1016/J.Clay.2015.01.028

[4] Andrew RM (2018) Global CO_2 Emissions From Cement Production. Earth System Science Data 10:195–217. Https://Doi.Org/10.5194/Essd-10-195-2018

[5] Artioli G, Secco M (2016) Modern And Ancient Masonry: Nature And Role Of The Binder. In: Brick And Block Masonry. CRC Press

[6] ASTM International (2021–2025) Standard Test Methods And Specifications For Concrete And Soil Materials. ASTM International, West Conshohocken, PA. Includes:
- ASTM E691 – Standard Practice For Conducting An Interlaboratory Study To Determine The Precision Of A Test Method
- ASTM D6913 – Standard Test Methods For Particle-Size Distribution (Gradation) Of Soils Using Sieve Analysis
- ASTM D4318 – Standard Test Methods For Liquid Limit, Plastic Limit, And Plasticity Index Of Soils
- ASTM D698 – Standard Test Methods For Laboratory Compaction Characteristics Of Soil Using Standard Effort
- ASTM D2166 – Standard Test Method For Unconfined Compressive Strength Of Cohesive Soi
- ASTM C1202 – Standard Test Method For Electrical Indication Of Concrete's Ability To Resist Chloride Ion Penetration
- ASTM C125-25a – Terminology Relating To Concrete And Aggregates
- ASTM C618-22 – Specification For Coal Fly Ash And Raw Or Calcined Natural Pozzolan For Use In Concrete
- ASTM C1556-21 – Standard Test Method For Determining The Apparent Chloride Diffusion Coefficient Of Cementitious Mixtures By Bulk Diffusion

[7] Ayininuola G, Adekitan O (2016) Characterization Of Ajebo Kaolinite Clay For Production Of Natural Pozzolan. International Journal Of Civil, Environmental, Structural, Construction And Architectural Engineering 10:1212–1219

[8] Ayininuola GM, Adekitan AI (2016) Pozzolanic Potentials Of Some Soil Samples From Southwestern Nigeria. Journal Of Civil Engineering Research 6(2):27–32

[9] Azad AK, Rasul MG, Khan MMK (2013) Comparative Assessment Of Energy Requirements And CO_2 Emissions Of Cement Production Using Alternative Fuels. International Journal Of Environmental Science And Technology 10(3):653–662. Https://Doi.Org/10.1007/S13762-012-0151-4

[10] British Standards Institution (1990) BS 1377: Methods Of Test For Soils For Civil Engineering Purposes. Parts 1–9. BSI, London

[11] British Standards Institution (1983) BS 1881-116: Method For Determination Of Compressive Strength Of Concrete Cubes. BSI, London

[12] British Standards Institution (2019) BS EN 12390-3: Testing Hardened Concrete – Part 3: Compressive Strength Of Test Specimens. BSI, London

[13] Cardoso TC, De Matos PR, Py L, Longhi M, Cascudo O, Kirchheim AP (2022) Ternary Cements Produced With Non-Calcined Clay,

Limestone, And Portland Clinker. Journal Of Building Engineering 45:103437. Https://Doi.Org/10.1016/J.Jobe.2021.103437
[14] Dayou ED, Zokpodo KLB, Glèlè Kakaï LR (2018) Assessment Of The Physical And Mechanical Properties Of The Soils In The Different Agroecological Zones Of Benin. Agro-Science 16:37. Https://Doi.Org/10.4314/As.V16i3.6
[15] Dodson VH (1990) Concrete Admixtures. Springer US, Boston, MA. Https://Doi.Org/10.1007/978-1-4757-4843-7
[16] Elsen J, Mertens G, Snellings R (2011) Portland Cement And Other Calcareous Hydraulic Binders: History, Production And Mineralogy. European Mineralogical Union Notes In Mineralogy 9:441–479. Https://Doi.Org/10.1180/EMU-Notes.9.11
[17] Geiker MR, Gallucci E (2019) Clays As SCM–Reactivity Of Uncalcined Kaolinite And Bentonite, And Impact On Phase Assemblage And Strength Development Of PC Mortars. Nordic Concrete Research 60:13–30. Https://Doi.Org/10.2478/Ncr-2019-0006
[18] Google Arts & Culture (N.D.) The Benin Moat. Https://Artsandculture.Google.Com/Asset/The-Benin-Moat/Vagnal5ypzecwa?Hl=En [Accessed 20 August 2025]
[19] Guo S, Wu Y, Jia Z, Qi X, Wang W (2023) Sodium-Based Activators In Alkali-Activated Materials: Classification And Comparison. Journal Of Building Engineering 70:106397. Https://Doi.Org/10.1016/J.Jobe.2023.106397
[20] Head KH (2006) Manual Of Soil Laboratory Testing: Volume 1 – Soil Classification And Compaction Tests. 3rd Edn. Whittles Publishing, Dunbeath
[21] Howtoconcrete.Com (2025) Concrete Curing Time Chart. Https://Howtoconcrete.Com/Concrete-Curing-Time-Chart [Accessed 20 August 2025]
[22] Ibrahim M, Rahman MK, Johari MAM, Maslehuddin M (2018) Effect Of Incorporating Nano-Silica On The Strength Of Natural Pozzolan-Based Alkali-Activated Concrete. In: Taha MMR (Ed) International Congress On Polymers In Concrete (ICPIC 2018). Springer International Publishing, Cham, Pp 703–709. Https://Doi.Org/10.1007/978-3-319-78175-4_90
[23] Idemudia M (2024) Rethinking The Global Prospects And Future Of The Historic Benin Moats In The Wake Of Urbanization. Journal Of African Studies And Sustainable Development 7(3). Https://Www.Apas.Africa/Journal_Article.Php?J=Jassd-550 [Accessed 20 August 2025]
[24] Iorfa TF, Iorfa KF, Mcasule AA, Akaayar MA (2020) Extraction And Characterization Of Nanocellulose From Rice Husk. SSRG International Journal Of Applied Physics 7:117–122. Https://Doi.Org/10.14445/23500301/IJAP-V7I1P117
[25] Istock (2025) Stock Photo Of Traditional Hut [Photograph]. Stock File ID: 1290323614. Https://Www.Istockphoto.Com [Accessed 20 August 2025]
[26] Iravanian A, Kassem Y, Gökçekuş H (2022) Stress–Strain Behavior Of Modified Expansive Clay Soil: Experimental Measurements And Prediction Models. Environmental Earth Sciences 81:1–17. Https://Doi.Org/10.1007/S12665-022-10229-8
[27] Kpade L, Akinyemi LP, Akinyemi FO, Olanrewaju RM (2022) Development Of A Digital Soil Fertility Index Map For Benin Using Machine Learning And Available Soil Data. Land 11(12):2155. Https://Doi.Org/10.3390/Land11122155
[28] Makusa GP (2012) Soil Stabilization Methods And Materials In Engineering Practice. Luleå University Of Technology, Department Of Civil, Environmental And Natural Resources Engineering. Https://Www.Diva-Portal.Org/Smash/Get/Diva2:997144/FULLTEXT01.Pdf [Accessed 20 August 2025]
[29] Mitchell J, Soga K (2005) Fundamentals Of Soil Behaviour. 3rd Edn. John Wiley & Sons, Hoboken, NJ
[30] Mota B, Matschei T, Scrivener K (2018) Impact Of Naoh And Na_2SO_4 On The Kinetics And Microstructural Development Of White Cement Hydration. Cement And Concrete Research 108:172–185. Https://Doi.Org/10.1016/J.Cemconres.2018.03.017
[31] Moussa RS, Mahamane A, Mahamane AI, Mahamane M, Mahamane A (2022) Physico-Chemical, Mineralogical And Structural Characterization Of A Clay Of Tanout (Zinder-Niger). World Journal Of Advanced Research And Reviews 16(2):1077–1092. Https://Doi.Org/10.30574/Wjarr.2022.16.2.1272
[32] Oyelade AO, Ayandeji AJ, Yekeen AA, Abiodun YO, Oribayo O (2025) Compressive Strength Prediction For Sandcrete Blocks With Metakaolin: Experiment And Multiple Linear Regression Analysis. Discover Civil Engineering 2:1–16. Https://Doi.Org/10.1007/S44290-025-00210-2
[33] Pachta V, Stefanidou M, Konopisi S, Papayianni I (2014) Technological Evolution Of Historic Structural Mortars. Journal Of Civil Engineering And Architecture 8:846–854. Https://Doi.Org/10.17265/1934-7359/2014.07.005
[34] Pinheiro VD, Alexandre J, Xavier GC, Marvila MT, Monteiro SN, De Azevedo ARG (2023) Methods For Evaluating Pozzolanic Reactivity In Calcined Clays: A Review. Materials (Basel) 16:4778. Https://Doi.Org/10.3390/Ma16134778
[35] Rashad AM (2023) A Concise On The Effect Of Calcium Oxide On The Properties Of Alkali-Activated Materials: A Manual For Civil Engineers. International Journal Of Concrete Structures And Materials 17(1):72. Https://Ijcsm.Springeropen.Com/Articles/10.1186/S40069-023-00635-Y [Accessed 20 August 2025]
[36] Scrivener K, John V, Gartner E (2018) Eco-Efficient Cements: Potential Economically Viable Solutions For A Low-CO_2 Cement-Based Materials Industry. Cement And Concrete Research 114. Https://Doi.Org/10.1016/J.Cemconres.2018.03.015
[37] Sherwood P (1993) Soil Stabilization With Cement And Lime: State-Of-The-Art Review. Transport Research Laboratory And H.M. Stationery Office, London
[38] Shi C (2001) An Overview On The Activation Of Reactivity Of Natural Pozzolans. Canadian Journal Of Civil Engineering 28(5):778–786. Https://Doi.Org/10.1139/L01-041 [Accessed 20 August 2025]
[39] Wang D, Wang Z, Wang H (2024) Feasibility And Performance Assessment Of Novel Framework For Soil Stabilization Using Multiple Industrial Wastes. Construction And Building Materials. Https://Www.X-Mol.Com/Paper/1835583223838781440?Adv [Accessed 20 August 2025]
[40] Wenapere DA, Ephraim ME (2009) Physico-Mechanical Behaviour Of Sandcrete Block Masonry Units. Journal Of Building Appraisal 4:301–309. Https://Doi.Org/10.1057/Jba.2009.8
[41] Gross J, Adaska W (2020) Guide To Cement-Stabilized Subgrade Soils. Portland Cement Association And National Concrete Pavement Technology Center, Iowa State University. Https://Www.Cptechcenter.Org/Wp-Content/Uploads/2020/05/Guide_To_CSS_Tablet.Pdf [Accessed 20 August 2025]
[42] NBC (2006) National Building Code Of Nigeria. Federal Ministry Of Works And Housing
[43] Ontario Building Code (2012) O. Reg. 332/12: Building Code. Government Of Ontario
[44] Pan Y, Chen M, Chen Y (2025) Analysis Of The Relationship Between Soil Particle Fractal Dimension And Physicochemical Properties. Environmental Earth Sciences 84:200. Https://Doi.Org/10.1007/S12665-025-12214-3
[45] Zhang H, Wang C, Chen Z, Kang Q, Xu X, Gao T (2022) Performance Comparison Of Different Particle Size Distribution Models In The Prediction Of Soil Particle Size Characteristics. Land 11(11):2068. Https://Doi.Org/10.3390/Land11112068